SOME INSIGHTS INTO THE DYNAMIC RESPONSE OF FLEXIBLE ROTORS SUPPORTED ON FLUID FILM BEARINGS

Wéderley Mendes Miranda
Departmento de Engenharia Mecanica
Universidade Federal de Minas Gerais
wederley@yahoo.com.br

Luiz Henrique Jorge Machado
Departmento de Engenharia Mecanica
Universidade Federal de Minas Gerais
luiz_machado@yahoo.com.br

Marco Tulio C. Faria
Departmento de Engenharia Mecanica
Universidade Federal de Minas Gerais
Av. Antonio Carlos, 6627
31270-901 – Belo Horizonte, MG - Brasil
mtcdf@uol.com.br

Abstract. *This paper presents the development of a finite element procedure specially devised to analyze the unbalance response of flexible rotors running on fluid film bearings. The shaft finite element model is based on the Timoshenko beam theory, which includes the elastic contribution from the shear effects and the inertial contribution from the rotary inertia and gyroscopic moments. Moreover, a finite element procedure for solution of the classical Reynolds equation for incompressible fluid films, in conjunction with a linearized perturbation procedure, is implemented to allow the computation of the dynamic force-coefficients of cylindrical journal bearings. The finite element equations of motion for an unbalanced rotor supported on fluid film bearings are integrated by using the Newmark method. The procedure permits the determination of the the time-domain and frequency-domain unbalance response of rotor-bearing systems at different journal loads and eccentricities. Numerical results depict some curves of whirl amplitude versus frequency and some plots of the whirl orbit for a rotor composed of a flexible shaft and an unbalanced rigid disk supported on two hydrodynamic journal bearings. The effects of the cross-coupled bearing stiffness and damping on the rotor unbalanced response are analyzed by using the computational procedure implemented in this work.*

Keywords*: Flexible Rotors; Journal Bearings; Rotor-Bearing Systems; Finite Element; Unbalance Response*

1. Introduction

Analysis, design and commissioning of all rotating machines require careful execution, in order to allow safe operation and efficiency in energy consumption. Researchers have been continuously devising experimental, analytical and computational procedures to analyze the several dynamic aspects associated with rotating shafts employed on high-speed machines. Since 1970, the finite element method has been largely used to develop models for flexible rotors and to perform analyses of balancing, stability and torsional vibration of rotating machinery (Childs, 1993; Vance, 1998; Nelson and McVaugh, 1976; Zorzi and Nelson, 1977; Nelson, 1980). For a rotating shaft, the Timoshenko beam theory has been employed to build finite element models very accurate to analyze the dynamics of flexible rotors (Nelson, 1980).

Computational procedures able to predict the unbalance response of high-speed rotors supported on fluid film bearings have been the goal of many turbomachinery manufacturers (Busse *et al*., 1980). Those procedures are very useful in the preliminary design stages and in the commissioning of industrial rotating machines employed in the oil industry and in petrochemical plants. To improve the capability of predicting the intricate dynamic phenomena in turbomachinery, experimental procedures have been developed to analyze, troubleshoot and monitor rotating machines (Schlegel, 1984). Techniques for measurement, troubleshooting and monitoring in rotordynamics has heavily relied on intensive experiments and tests performed on rotor-bearing testing benches (Machado *et al*. 2004). Moreover, experimental data have provided very useful information to enlarge the capabilities of computer codes available for dynamic analyses of flexible rotors.

This paper deals with the dynamic analysis of flexible rotors supported on oil-lubricated journal bearings. A finite element procedure is specially devised to compute the unbalance response of rotating shafts supported on hydrodynamic bearings. The Timoshenko beam theory is applied to carry out the rotating shaft finite element modeling, accounting for the shear effects, the gyroscopic moments and the rotatory inertia. Lumped masses are used to model disks and impellers attached to the rotating shaft. Hydrodynamic journal bearing finite element modeling is based on the classical Reynolds equation. A linearized perturbation method is applied on the Reynolds equation to render the lubrication

equations capable of predicting the eight linearized dynamic force coefficients associated with the bearing stiffness and damping. Experimental results for vibration spectra obtained on a horizontal test rig, which comprises of a multi-disk rotating shaft supported on two hydrodynamic cylindrical journal bearings, are employed to adjust the computational procedure implemented in this work. Predicted unbalance response for some rotor configurations is compared with experimental curves. Numerical results are computed for both the frequency-domain unbalance response and the journal center whirl orbits at different operating conditions. The influence of the bearing dynamic force coefficients on the dynamic response of flexible rotors is shown on the curves presented in this work. The effective damping of rotor-bearing systems is demonstrated to be a very important design parameter for high-speed rotating machinery.

2. Finite element procedure

The rotor-bearing system is modeled using finite element models for both the flexible shaft and the hydrodynamic journal bearings. The finite element equations of motion are solved by using the Newmark method (Bathe, 1982). Figure 1 depicts a schematic view of a flexible rotor supported on fluid film journal bearings. At this item, the implementation steps of the finite element procedure are described.

2.1. Shaft modeling

The finite element shaft modeling implemented in this work has been based on the special shape functions derived by Nelson (1980). Nelson (1980) employs the Timoshenko beam theory to derive the equilibrium equations for a flexible circular shaft supported on elastic supports taking into account the shaft shear effects, gyroscopic moments and rotatory inertia. The system is represented schematically in Fig.1.

Two node beam elements with eight degrees-of-freedom are employed to model the lateral motion of flexible shafts. The journal bearing contributions to the rotor stiffness and damping coefficients are accounted for. The finite element procedure is based on the following global equation of motion:

$$[\mathrm{M}+\mathrm{N}]\{\ddot{\mathrm{U}}\}+[\mathrm{C}]\{\dot{\mathrm{U}}\}+[\mathrm{K}]\{\mathrm{U}\}=\{\mathrm{R}\} \tag{1}$$

where, $[M]$ represents the global shaft translational inertia matrix, $[N]$ represents the global rotatory inertia matrix, $[K]$ the shaft and bearing stiffness matrix and $[C]$ is the generalized shaft and bearing damping matrix, which is expressed as $[\mathrm{C}]=[\mathrm{C}_1]-\Omega[\mathrm{G}]$, in which $[G]$ is the shaft gyroscopic effects matrix. The matrix $[\mathrm{C}_1]$ represents the bearing damping. The shaft acceleration, velocity and displacement vectors are given, respectively, by $\{\ddot{\mathrm{U}}\},\{\dot{\mathrm{U}}\},\{\mathrm{U}\}$, and Ω is the shaft rotating speed (rad/s).

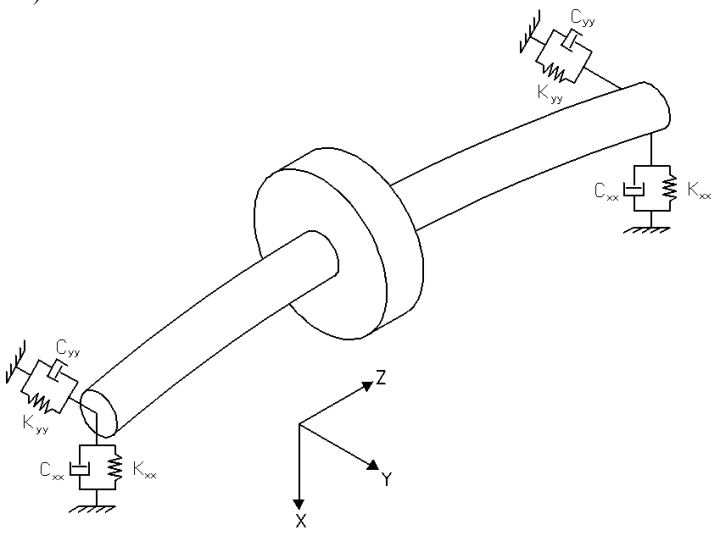

Figure 1. Flexible shaft supported on fluid film journal bearings.

The rotor unbalance load is represented by the vector {R} on Eq. (1). A rotating unbalanced rigid disk is mounted at pre-determined axial shaft positions to allow the load application. A rotating phasor with amplitude of $F_0 = \mathrm{m_d}.\mathrm{u_d}.\ \Omega^2$, represents the mass unbalance load, in which m_d is the unbalance mass (kg) and u_d is the unbalance mass eccentricity (m). A hypothetical mass eccentricity is used to introduce the unbalance load into the finite element model. The Newmark method is employed to solve the second-order differential equation (1) (Bathe, 1982).

2.2. Bearing modeling

The journal bearing finite element model is developed based on the classical Reynolds equation for oil-lubricated cylindrical journal bearings (Childs, 1993). For the coordinates (*X*,*Z*), this equation is given by.

$$\frac{\partial}{\partial X}\left(\frac{h^3}{12\mu}\frac{\partial P}{\partial X}\right)+\frac{\partial}{\partial Z}\left(\frac{h^3}{12\mu}\frac{\partial P}{\partial Z}\right)=\frac{\Omega R}{2}\frac{dh}{dX}+\frac{\partial h}{\partial t} \tag{2}$$

The journal rotational speed is denoted by Ω. Journal eccentricities in the vertical and horizontal directions are expressed as e_X and e_Y, respectively. The eccentricity ratio is defined as $\varepsilon = e/c$, where $e^2=e_X^2+e_Y^2$. The circumferential coordinate $X = R.\theta$ and R is the bearing radius. Fluid viscosity is given by μ, P represents the hydrodynamic pressure and h is the fluid film thickness. A linearized perturbation procedure is used in conjunction with Eq. (2) to render the zeroth- and first-order lubrication equations (Faria, 2001). These equations, which are shown below, allow the computation of the bearing reaction forces and eight dynamic force coefficients.

$$\frac{\partial}{\partial X}\left(\frac{h^3}{12\mu}\frac{\partial P}{\partial X}\right)+\frac{\partial}{\partial Z}\left(\frac{h^3}{12\mu}\frac{\partial P}{\partial Z}\right)=-\frac{\Omega R}{2}\frac{dh_0}{dX}-\Omega\{e_{X0}\sin(\theta+\Omega.t)-e_{Y0}\cos(\theta+\Omega.t)\} \tag{3}$$

$$\frac{\partial}{\partial X}\left(\frac{h^3}{12\mu}\frac{\partial P}{\partial X}\right)+\frac{\partial}{\partial Z}\left(\frac{h^3}{12\mu}\frac{\partial P}{\partial Z}\right)=-\frac{\Omega R}{2}\frac{dh_\sigma}{dX}+\mathbf{i}\omega h_\sigma+\Omega R\frac{dh_\sigma}{dX}-\frac{\partial}{\partial X}\left(\frac{3h_0^2h_\sigma}{12\mu}\frac{\partial P_0}{\partial X}\right)-\frac{\partial}{\partial Z}\left(\frac{3h_0^2h_\sigma}{12\mu}\frac{\partial P_0}{\partial Z}\right) \tag{4}$$

In these equations, h_0 denotes the zeroth-order film thickness and h_σ represents the first-order perturbed thickness. The perturbation is applied at the excitation frequency ω on an equilibrium position (e_{X0}, e_{Y0}). P_0 represents the zeroth-order pressure and $\{P_\sigma\}$, σ = *X, Y*, represent the pressure field caused by the dynamic perturbations of rotor displacements and velocities. The bearing dynamic force coefficients are estimated using a finite element procedure that is able to compute the dynamic bearing characteristics from the zeroth- and first-order pressure fields (Faria, 2000). The bearing dynamic coefficients associated with the stiffness $\{K_{\sigma\beta}\}_{\beta,\sigma=X,Y}$ and damping $\{C_{\sigma\beta}\}_{\beta,\sigma=X,Y}$ are calculated from the complex impedances in the following form

$$Z_{\sigma\beta}=K_{\sigma\beta}+i\omega C_{\sigma\beta}=-\int_0^L\int_0^{2\pi}p_\beta h_\sigma R.d\theta.dz\;;\quad \beta,\sigma=X,Y \tag{5}$$

or

$$\begin{bmatrix}K_{XX} & K_{XY}\\ K_{YX} & K_{YY}\end{bmatrix}+i.\omega.\begin{bmatrix}C_{XX} & C_{XY}\\ C_{YX} & C_{YY}\end{bmatrix}=-\int_0^L\int_0^{2\pi}\begin{bmatrix}p_Xh_X & p_Yh_X\\ p_Xh_Y & p_Yh_Y\end{bmatrix}.R.d\theta.dz\,.$$

The stiffness $[K_m]$ and damping $[C_m]$ represent the fluid film resistance to the rotor displacement and velocity, respectively. They are defined as.

$$[\mathrm{K_m}]=\begin{bmatrix}K_{XX} & K_{XY}\\ K_{YX} & K_{YX}\end{bmatrix}\qquad [\mathrm{C_m}]=\begin{bmatrix}C_{XX} & C_{XY}\\ C_{YX} & C_{YX}\end{bmatrix} \tag{6}$$

Figure 2 shows the cross-section of a journal bearing, in which there are eight linearized stiffness and damping coefficients representing the dynamic characteristics of the bearing thin fluid film.

3. Numerical results

3.1. Validation

The finite element procedure developed in this work is able to determine the unbalance response of flexible rotors supported on oil-lubricated journal bearings. The computation of the dynamic force coefficients for cylindrical journal bearings is validated by comparing the finite element results for bearing damping and stiffness with the theoretical results obtained from the short journal bearing model (Chidls, 1993). For brevity, the validation of the finite element procedure for the bearing dynamic coefficients are omitted in this work.

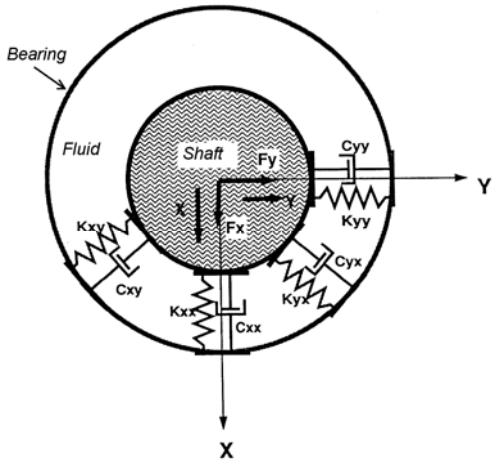

Figure 2. Linearized stiffness and damping coefficients of the journal bearing

To validate the finite element procedure for the rotor-bearing system, numerical predictions of frequency spectra for an example of rotor are compared with experimental data. Table 1 shows the rotor parameters of a rotor test rig, which has been built to test different journal bearing configurations for horizontal rotors. The experimental setup is assembled with adjustable two bearing pedestals in one fixed base, which allow to vary the rotor length. One or two unbalance circular discs can be mounted on the rotating shaft to simulate real mass unbalance conditions.. An electric motor is used to drive the horizontal rotor through a transmission system comprised of pulleys and belt. A frequency inverter has been used to control de rotor speed and impose different time rates for the rotating system acceleration and deceleration (Machado *et al*., 2004). Table1 presents the constitutive and operating parameters employed on the rotor test rig. Figure 3 depicts a schematic view of the experimental apparatus of the test rig.

Table 1. Experimental Rotor-Bearing Parameters

D (shaft diameter) = 0.015 m	μ (lubricant viscosity) = 25 x 10^{-3} Pa·s
L (bearing length) = 0.012 m	ρ (lubricant density)= 892 kg/m³
c_1 (bearing 1 radial clearance) = 34.5 μm	number of finite elements of shaft elements = 80
c_2 (bearing 2 radial clearance) = 77.5 μm	l (shaft length between bearings) = 0.30 m
Ω (rotor speed) = 0 to 10,000 rpm	

The experimental frequency spectra have been obtained for different shaft speed for the rotor supported on hydrodynamic cylindrical journal bearings by bump tests and rotation tests. The experimental study used accelerometers and frequency spectra analyzer. The accelerometers are placed on the top of the two bearing pedestals. The rotor speed varies from 700 to 9,800 rpm during the experimental vibration tests. The frequency analyzer used to obtain the frequency-domain dynamic response is the Hewlett Packard HP 350670A in conjunction with a pair of commercial accelerometers.

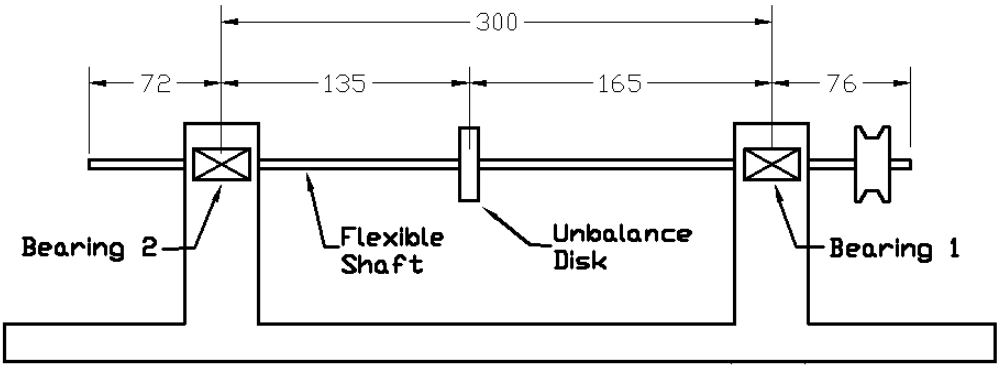

Figure 3. Experimental setup for testing rotating shafts supported on fluid film bearings.

In order to obtain the numerical unbalance response, a small unbalance mass is used to generate an excitation force on the rotor. Some adjustments are performed on the bearing dynamic force coefficients to fit the rotor model following the experimental data available.

Firstly, a comparison of experimental frequency spectra with predicted results is performed to validate the finite element procedure developed in this work. Figure 4 shows the experimental frequency-domain vibratory response of the rotor depicted in Fig. 3 during some bump tests. This curve is plotted for RMS values of acceleration. Experimental data have been collected by different tests, with the vibration sensor on bearing 1 and bearing 2, and bumping on both sides of the shaft. Two peaks are obtained at the frequencies approximately of 83 Hz (5000 rpm) and 110 Hz (6600 rpm). Figures 5, 6 and 7 depict the frequency-domain unbalance response amplitude computed by the finite element procedure at three rotating speeds. A peak at approximately 83 Hz in shown in Fig. 5, while Figs. 6 and 7 present a peak at approximately 110 Hz. These two peaks are associated with two natural frequencies of test rig rotor.

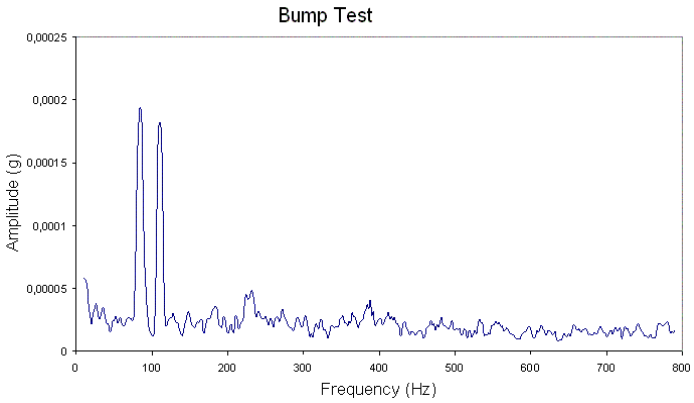

Figure 4. Frequency spectrum for bearing 1 generated by bumping the system at bearing 1.

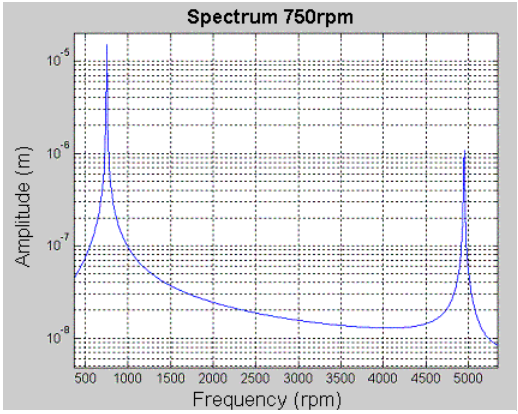

Figure 5. Predicted frequency spectrum for the bearing 1 response at 750 rpm.

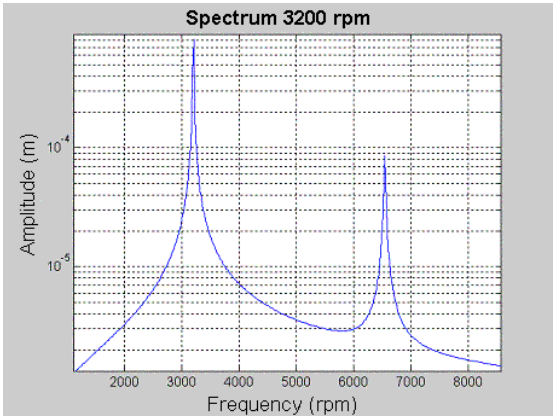

Figure 6. Predicted frequency spectrum for the bearing 1 response at 3200 rpm

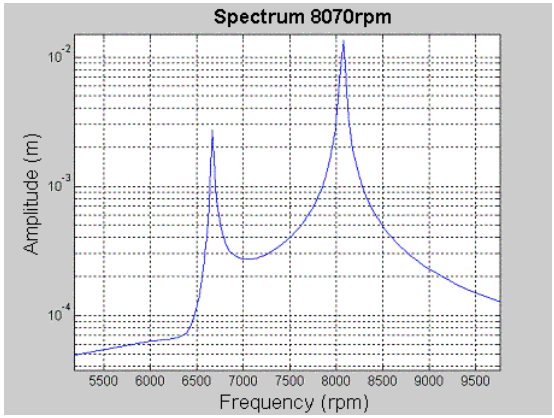

Figure 7. Predicted frequency spectrum for the bearing 1 response at 8070 rpm

Secondly, a second part of the validation is carried out by comparing the predicted spectra with experimental spectra for the rotor running at speed of 8,890 rpm. The responses are illustrated in Figs. 8 and 9, where some peaks at similar frequencies are displayed. This comparison shows that the finite element model reproduces important vibration frequencies of the test rig, exhibited in the experimental spectrum.

3.2. Rotor-bearing dynamic analysis

This section describes the numerical results obtained for the rotor whirl orbit at different operating conditions. The influence of the bearing cross-coupled stiffness and damping on the dynamic response of flexible rotors supported on hydrodynamic cylindrical journal bearings is analyzed through several plots of rotor whirl orbits.

The following examples show different situations where the stable equilibrium can be reached easily by increasing the bearing damping. The stability is related to the direct damping coefficients and cross-coupled stiffness by the expression $\frac{2\,\Omega\,C_{XX}}{K_{XY}}$ (Vance, 1988), where C_{xx} is the direct damping coefficient (or C_{yy}) and K_{xy} is the cross-coupled stiffness (or $-K_{yx}$).

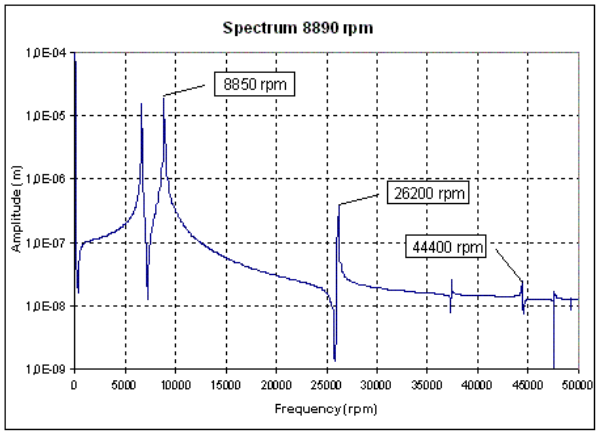

Figure 8. Predicted frequency spectrum for the bearing 1 response at 8,890rpm.

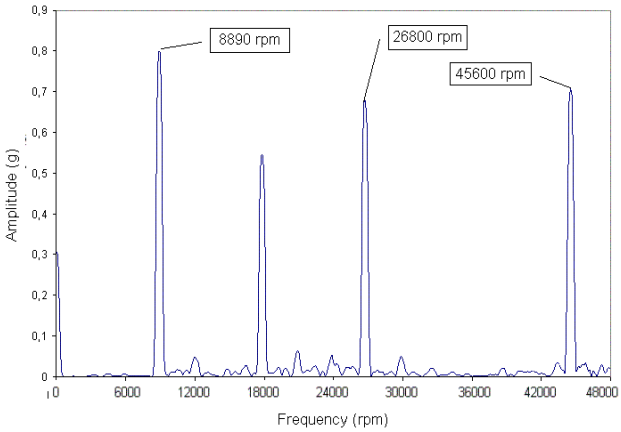

Figure 9. Experimental frequency spectrum for the bearing 1 response at 8,890rpm.

Figures 10 to 13 show the path of the journal center starting from the bearing center (position 0,0) for different values of $2\Omega C_{xx}/K_{xy}$. For small values of $2\Omega C_{xx}/K_{xy}$, normally under 1, the system is unstable, but this instability can be eliminated by increasing the direct damping coefficient, when the path of journal center rapidly approaches the static equilibrium position.

Figure 10 and 11 present the rotor whirl orbits for the system at 750 rpm shaft speed. Figure 10 shows the instability of the system when $2\Omega C_{xx}/K_{xy} = 0.1$. For such small value of effective damping, the rotating shaft supported by fluid film bearings usually becomes unstable. This instability can be controlled by increasing the damping, by making $2\Omega C_{xx}/K_{xy}$ larger. Figure 11 depicts the same system with the value of $2\Omega C_{xx}/K_{xy} = 5$, where the stability was clearly achieved.

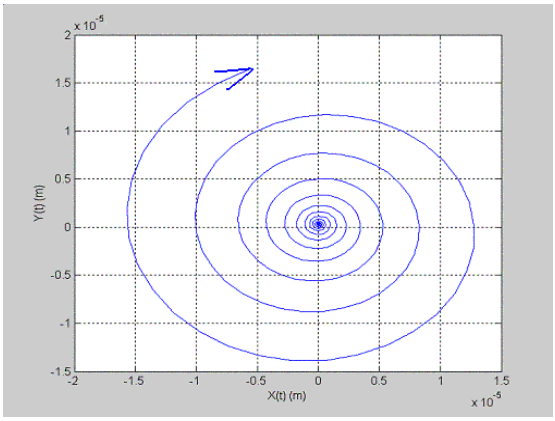

Figure 10. Journal center trajectory for an unstable example at 750rpm and $2\Omega C_{xx}/K_{xy} = 0.1$.

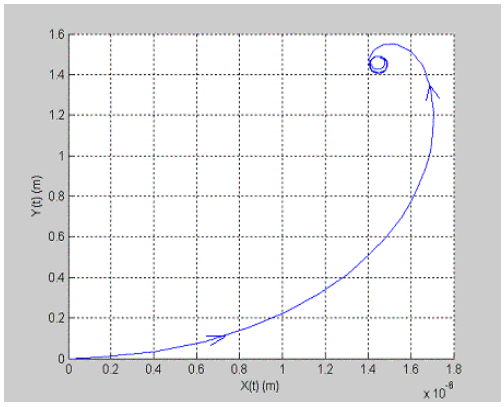

Figure 11. Journal center trajectory for a stable example at 750rpm and $2\Omega C_{xx}/K_{xy} = 5$.

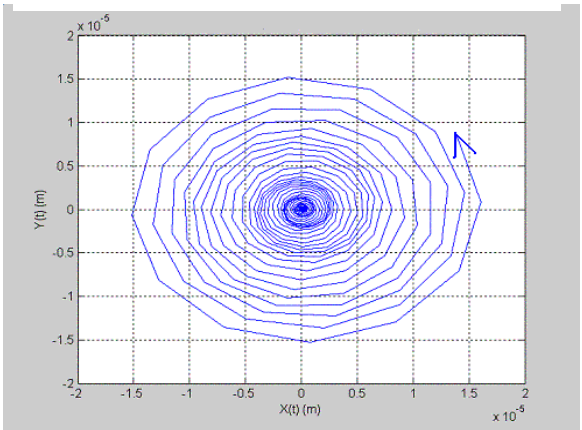

Figure 12. Journal center trajectory for an unstable example at 2400rpm and $2\Omega C_{xx}/K_{xy} = 0.1$.

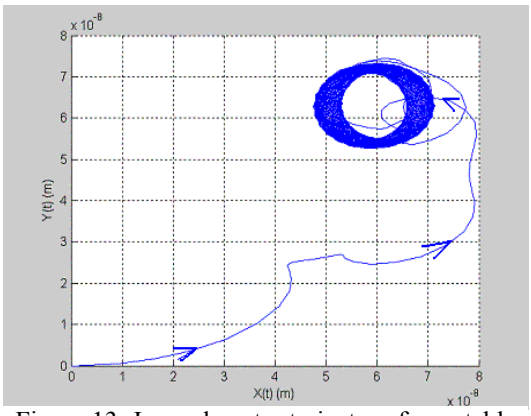

Figure 13. Journal center trajectory for a stable example at 2400rpm and $2\Omega C_{xx}/K_{xy} = 10$.

The same kind of analysis is carried out for the system at 2,400 rpm and shown in Fig. 12 and 13. The instability that occurs at $2\Omega C_{xx}/K_{xy} = 0.1$ (Fig.12) is eliminated by increasing the damping as shown in Fig. 13, where $2\Omega C_{xx}/K_{xy} = 10$. The distortions that appear on the orbits depicted on Fig. 12 are due to the large step increment used to compute the time response.

For the system at 4,000 rpm, the instability occurs for $2\Omega C_{xx}/K_{xy} = 1$ (Fig. 14) and it is eliminated by increasing the damping sufficiently to reach $2\Omega C_{xx}/K_{xy} = 2$, as shown in Fig.15. This is a typical example of limit-cycle stability.

Figure 14. Journal center trajectory for an unstable example at 4,000rpm and $2\omega C_{xx}/K_{xy}=1$.

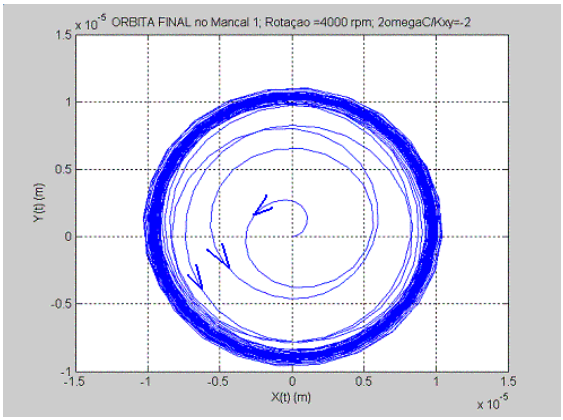

Figure 15. Journal center trajectory for a stable example at 4,000rpm and $2\omega C_{xx}/K_{xy} = 2$.

Time-domain unbalance response of rotor-bearing system at 4,800rpm are predicted at different journal journal eccentricity ratios (ε) and illustrated in Fig. 16. A hypothetical eccentricity at *x*-axis direction (vertical direction) has been established in order to verify the behavior of the rotor orbits and the stability of the system. The system under analysis is shown to be stable for all conditions analyzed, and the shaft center moves along a limit-cycle, as in Fig.15.

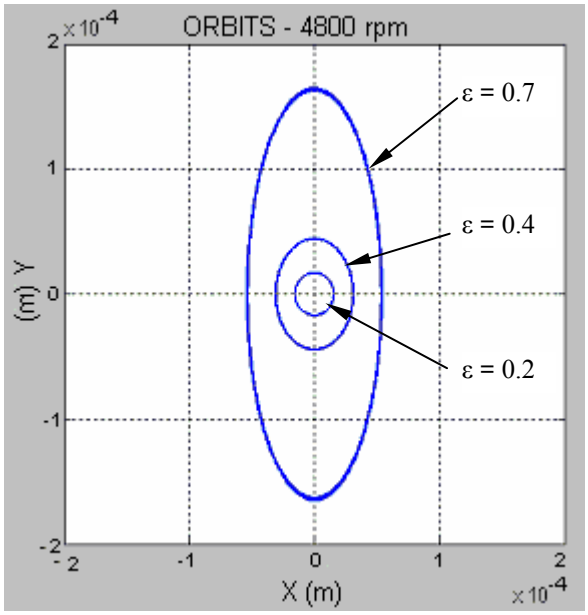

Figure 16. Orbits at 4800rpm for different values of journal eccentricity ratios (ε).

4. Conclusions

This paper presents a finite element procedure specially devised to analyze the unbalance response of high-speed rotors supported on hydrodynamic journal bearings. The computational accuracy of this procedure is demonstrated by comparing the pattern of the predicted rotor responses with that obtained through vibration tests carried out on a rotor test rig. This procedure can be very useful not only in the determination of the unbalance response of rotors employed in

industrial turbomachinery but also to evaluate feasible design changes capable of improving the machine dynamic behavior.

A very important stage in the design and commissioning of industrial rotating machines consists on the design of the rotor supporting system. Dynamic force coefficients play a crucial role in the rotor capability to bear undesirable vibrations and to run under stable conditions. The results presented in this work shows clearly the importance of selecting the more appropriate bearing configuration that can provide enough effective damping to bound the growth of the vibration response at critical operating conditions.

5. References

Bathe, K.J., 1982, 'Finite Element Procedures in Engineering Analysis", Prentice-Hall, Englewood Cliffs, USA, 734 p.

Busse, L., Heiberger, D. and Wey, J., 1980, "Aspects of Shaft Dynamics for Industrial Turbines", Brown Boveri Review, Vol. 67, pp. 292-299.

Childs, D.W., 1993, "Turbomachinery Rotordynamics", McGraw-Hill, New York, USA, 476 p.

Faria, M.T.C., 2000, "JBEARING: Program Listing and Manual", Research Notes, Departamento de Engenharia Mecânica, Universidade Federal de Minas Gerais, Belo Horizonte, Brazil.

Faria, M.T.C., 2001, "Some Performance Characteristics of High Speed Gas Lubricated Herringbone Groove Journal Bearings", JSME International Journal, Ser. C, Vol.44, pp. 775-781.

Nelson, H.D. , 1980, "A Finite Rotating Shaft Element Using Timoshenko Beam Theory", ASME Journal of Mechanical Design, Vol.102, pp. 793-803.

Nelson, H.D. and McVaugh, J.M., 1976, "The Dynamics of Rotor-Bearing Systems Using Finite Elements", ASME Journal of Engineering for Industry, May 1976, p. 593-600.

Machado, L.H.J., Silva, L.F.A.T. and Faria, M.T.C., 2004, "Design and Development of a Test Rig for Rotors and Journal Bearings", Proceedings of the third Seminar of the Research Center of Hydraulics and Hydric Resources (III Semin-CPH), Federal University of Minas Gerais, Belo Horizonte, Brazil, pp. 1-4.

Schlegel, V., 1984, "Vibration Measurement and Monitoring in Dynamics of Rotors – Stability and System Identification", Edited by O. Mahrenholtz, Springer-Verlag, EUA, pp. 333-351.

Vance, J.M., 1988, "Rotordynamics of Turbomachinery", McGraw-Hill, New York, USA, 370 p.

Zorzi, E.S. and Nelson, H.D., 1977, "Finite Element Simulation of Rotor-Bearing Systems With Internal Damping", ASME Journal of Engineering for Power, pp. 71-76.

6. Responsibility notice

The authors are the only responsible for the printed material included in this paper.

7. Acknowledgments

The financial support provided by the Brazilian Agency CNPq (Process N$^{o.}$ 472206/2001-0) and UFMG are gratefully acknowledged by the authors.